Prediction of Significant Tokamak Turbulence at Electron Gyroradius Scales

F. Jenko[1] and W. Dorland[2]

[1]*Max-Planck-Institut für Plasmaphysik, EURATOM Association, Boltzmannstrasse 2, 85748 Garching, Germany*
[2]*Imperial College, London SW7 2AZ, United Kingdom*

(Received 9 May 2002; published 7 November 2002)

The experimental conditions under which tokamak turbulence at hyperfine (electron gyroradius) scales is predicted to be significant and observable are described. The first quantitative predictions of fluctuation amplitudes, spectral features, and the associated electron energy transport are presented. A novel theoretical model which quantitatively describes the boundaries of the high-amplitude streamer transport regime is presented and shown to explain the gyrokinetic simulation results. This model uniquely includes consideration of two distinct secondary instabilities.

DOI: 10.1103/PhysRevLett.89.225001 PACS numbers: 52.35.Ra

The cross-field electron heat transport in magnetized fusion plasmas is generally found to be large compared to collision-driven fluxes, a fact attributed to turbulence driven by microinstabilities. Among the latter are ion temperature gradient (ITG) modes and trapped electron modes (TEMs), which are characterized by $k_\perp \rho_i \lesssim 1$ and may contribute to electron energy losses with a diffusion coefficient $\chi_e \sim \rho_i^2 v_{ti}/L$ [1], where $k_\perp$ is a typical perpendicular wave number of the turbulence, ρ_i is the ion gyroradius, v_{ti} is the ion thermal speed, and L is a typical perpendicular gradient scale length. Here, we focus on turbulent heat transport by electron temperature gradient (ETG) modes on much smaller scales, $k_\perp \rho_i \gg 1$. Although it has been previously established that ETG turbulence *could* be experimentally relevant [2,3], no quantitative predictions exist for either the transport level or the fluctuation amplitudes (and their spectral properties). Moreover, realistic experimental conditions under which one should expect ETG turbulence to be significant have not been outlined. In this Letter, we present the first predictions in each of these areas. We also present a theoretical model which successfully predicts key features of our nonlinear gyrokinetic ETG simulations. This relatively simple model of ETG turbulence dynamics may be a useful starting point for understanding a broad range of turbulence problems.

The linear theory of the toroidal ETG mode is well known [4]. Here, we find it useful to highlight the role of parallel velocity fluctuations in two extreme limits. In the first, curvature can be neglected. This "slab" mode has a small but finite parallel wave number ($0 < k_\parallel \ll k_\perp$) which couples temperature fluctuations to potential fluctuations via parallel electron dynamics. The linear eigenmode therefore has an intrinsic parallel velocity component. In the opposite limit, the temperature and potential fluctuations are coupled by perpendicular compressibility. To lowest order, one can consider $k_\parallel = 0$. As a result, this "curvature-driven" eigenmode does not have a significant parallel velocity component. For realistic parameters, neither limit exactly pertains. For example, the curvature-driven mode typically obtains a ballooning character, which reintroduces modest parallel velocity.

A key result of this paper is that the *nonlinear* development of an ETG instability is profoundly affected by its parallel velocity component, which determines which of two *distinct* nonlinear processes leads to saturation. The curvature-driven mode is broken up by a secondary (hereafter, "Rogers") instability that is driven by the perpendicular shear in the eigenmode's perpendicular $\mathbf{E} \times \mathbf{B}$ flow [2,3]. Because the Rogers secondary is dramatically weakened by the adiabatic ion response for $k_\perp \rho_i \gg 1$, a purely curvature-driven ETG mode tends to saturate at a high level compared to "mixing length" [5] expectations. Upon defining the latter as $\Phi_{\mathrm{ML}} \equiv (e\phi/T)_{\mathrm{ML}} \sim 1/[k_\perp (RL)^{1/2}]$, one may write $\Phi_{\mathrm{curv}} \sim \Phi_{\mathrm{ML}}/(k_\perp \rho_e)^2$, where a value of $k_\perp \rho_e \sim 0.1$–0.2 is typical [2,3]. This estimate comes from balancing the primary and secondary growth rates. (Here, Φ is the rms electrostatic potential, R is the major radius of the toroidal device, and ρ_e is the electron gyroradius.) Thus, ETG

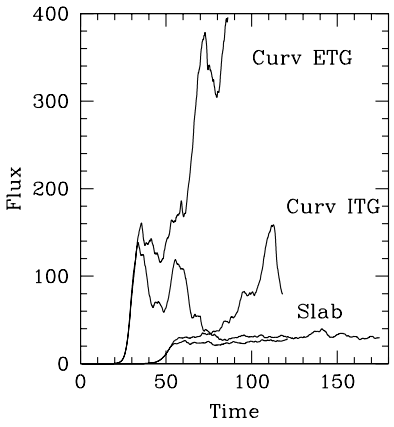

FIG. 1. Qualitative behavior of the heat flux as the adiabatic response is changed (ETG vs ITG), and as the instability drive is changed (parallel compression "Slab" vs perpendicular compression "Curv"). For $t > 90$, the flux from the curvature-induced ETG mode continues to grow.

turbulence arising mainly from curvature drive can induce electron thermal transport comparable to that induced by ITG modes and TEMs. Perpendicular shear in the *parallel* flow of the linear instability, on the other hand, drives a distinct (hereafter, "Cowley") secondary, described in detail in Ref. [6]. Importantly, for $k_\perp \rho_i \gg 1$, this secondary is not weakened by the ion response. (That is, while both secondaries have growth rates proportional to the primary's amplitude, the Cowley secondary has a much larger constant of proportionality when $k_\perp \rho_i \gg 1$.) Thus, at ρ_e scales, the Cowley secondary efficiently breaks up linear modes which contain intrinsic and substantial perpendicular gradients of parallel flows.

The importance of the different primary and secondary instabilities is demonstrated in Fig. 1. The ETG and ITG simulations differ only in the details of the adiabatic species' responses [2,3]. In the sheared slab cases (no curvature), the ETG and ITG simulations saturate at similar normalized levels. This occurs because the saturation mechanism is the Cowley secondary, which is not sensitive to the details of the adiabatic species' responses. In the cases labeled "Curv," we set the curvature to a constant value characteristic of the curvature at the outboard midplane of a conventional tokamak. The resulting linear instability is the curvature-driven branch, with no significant parallel compression. This eliminates the Cowley secondary. Detailed analysis of the simulation results shows that the linear modes are broken up by the Rogers secondary. The weakening of the Rogers secondary by the adiabatic ions allows the ETG simulation to go to much higher normalized amplitude and to exhibit streamers. To our knowledge, no other theoretical model of ETG or ITG turbulence predicts this striking behavior.

To study toroidal ETG turbulence under more realistic conditions, we use two independently developed codes, GENE and GS2, to solve the nonlinear electromagnetic gyrokinetic Vlasov-Maxwell equations [7] in magnetic flux-tube geometry [6,8], employing a fixed grid in five-dimensional phase space. Although both codes are designed to work in general tokamak geometry, we restrict ourselves in the present study to a large aspect ratio, circular flux surface magnetohydrodynamic model equilibrium [9] which is characterized by magnetic shear $\hat{s}$ and normalized pressure gradient α. The simulations are carried out in magnetic flux tubes with typical perpendicular dimensions of 128–$512\rho_e$ and box size ratios of $L_x/L_y = 1$–4. The ion response is taken to be purely adiabatic. Trapped electron effects, collisions, and electron Debye length effects are neglected. As numerical parameters we use 0.25–2 grid points per ρ_e in the perpendicular directions, 16–32 grid points along the parallel direction, and 25×10 points in $v_\parallel$-μ space. Convergence checks with respect to box size and numerical resolution have been performed. As standard parameters, we take $R/L_n = 2.2$, $R/L_{Te} = 6.9$, $q = 1.4$, $\tau \equiv Z_{\rm eff} T_e/T_i = 1$, and $\alpha = \beta = 0$, where L_n and L_{Te} are the density and electron temperature gradient scale lengths, respectively, β is the ratio of thermal to magnetic pressure, q is the safety factor, and $Z_{\rm eff}$ is an effective ion charge.

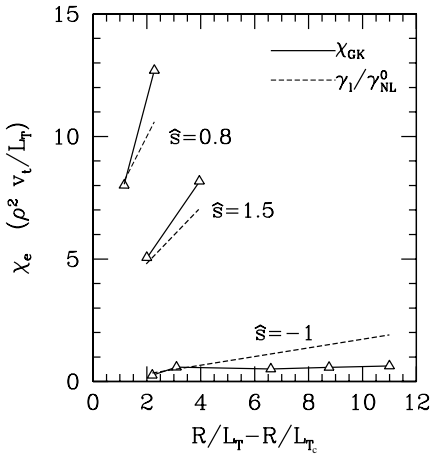

FIG. 2. Electron heat flux from nonlinear gyrokinetic simulations of ETG turbulence for our nominal parameters and $\hat{s} = 0.8$ ($R/L_{Tc} \sim 4.6$), $\hat{s} = 1.5$ ($R/L_{Tc} \sim 7.1$), and $\hat{s} = -1$ ($R/L_{Tc} \sim 6.3$), together with theoretical predictions.

The dependence of χ_e on R/L_{Te} for these parameters and three values of $\hat{s}$ is shown in Fig. 2. For moderate positive shear, $\hat{s} = 0.8$, χ_e rises quite strongly as soon as R/L_T exceeds the linear threshold, $R/L_{Tc} \equiv (R/L_{Te})_{\rm crit}$. In this case, the ETG turbulence is dominated by streamers, and χ_e exceeds the mixing length estimate by an order of magnitude or more. At higher $\hat{s}$, χ_e is less stiff but still clearly beyond mixing length expectations. However, for negative shear, $\hat{s} = -1$, the transport level drops down to the mixing length level and streamers are not observed. Typical density fluctuation spectra, $\Gamma_A = \sum_{k_y} \Gamma_A(k_y)$ [$\Gamma_A = A^2$, $A = (\tilde{n}_e/n_{e0})(L_n/\rho_e)$], from these simulations are shown in Fig. 3. Comparing cases with and without streamers, one observes a strong change in amplitude together with a modest shift of the position of the k_y peak. For $\hat{s} = 0.8$ ($\hat{s} = -1$), the spatially averaged fluctuation amplitudes are given by $\tilde{n}_e/n_{e0} \sim g\,(\rho_e/R)\,(R/L_{Te} - R/L_{Tc})$ with $g \sim 20$ ($g \sim 3$). Thus, streamer activity boosts $\tilde{n}_e/n_{e0}$ by about an order of magnitude and makes experimental detectability more likely. Figures 2 and 3 represent the first quantitative predictions of ETG turbulence properties. They are based on a large number of state-of-the-art, first-principles simulations on TFlop-scale supercomputers.

We now demonstrate the application of secondary instability theory to the problem of elucidating the physics of these simulations. The basic idea of the theory is to predict the saturation amplitude by balancing primary (γ_ℓ) and secondary ($\gamma_{\rm NL}$) growth rates. To do this, one must first calculate $\gamma_{\rm NL}$. At sufficiently high amplitude, $\gamma_{\rm NL} \propto \Phi_\ell$. We thus compute $\gamma^0_{\rm NL}$ by freezing a given linear eigenmode at a fiducial high amplitude

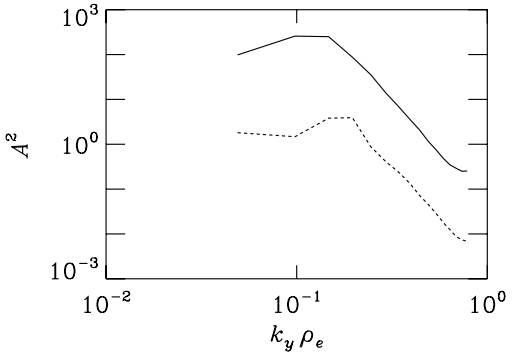

FIG. 3. Typical density fluctuation spectra from high (low) amplitude streamer-dominated (streamer-free) ETG turbulence for $\hat{s} = 0.8$ ($\hat{s} = -1$) shown as a solid (dotted) line. Here, $A \equiv (\tilde{n}_e/n_{e0})(L_n/\rho_e)$ and $R/L_{Te} - R/L_{Tc} \sim 2.3$.

($\Phi_\ell = \Phi_\ell^0$), and using this state as the "equilibrium" for a sequence of initial value calculations with varying k_x. This amounts to solving (as a function of k_x) the 2D eigenvalue problem for the secondary in the y, z plane of the coordinates that are twisting with the magnetic field. Given Φ_ℓ^0, $\gamma_{\rm NL}^0$, and γ_ℓ, the rms amplitude of Φ in the turbulent state is estimated by $\Phi/\Phi^0 = \gamma_\ell/\gamma_{\rm NL}^0$. (We note that all our results are in the strong turbulence regime, where $\chi_e \propto \Phi$, so that $\gamma_\ell/\gamma_{\rm NL}^0$ also roughly predicts the anomalous diffusion coefficient.)

We find that, for ETG modes, the ratio $\gamma_\ell/\gamma_{\rm NL}^0$ varies greatly, depending mainly on the nature of the secondary (Cowley vs Rogers). Apart from the growth rate, there are two key signatures which differentiate them. First, the structure of the secondary along the field line differs, as shown in Fig. 4. The Rogers secondary is localized to the maximum of the shear in the perpendicular flow (in this case, near $\theta = 0$) and has a small parallel wave number. (With constant curvature, $k_\parallel = 0$.) The Cowley secondary is localized to the region where there is a finite poloidal gradient of the parallel velocity and zero perpendicular velocity, and has a large parallel wave number that is directly proportional to the amplitude of the primary. Second, the $k_x/k_y^{(\ell)}$ spectra (not shown) are very

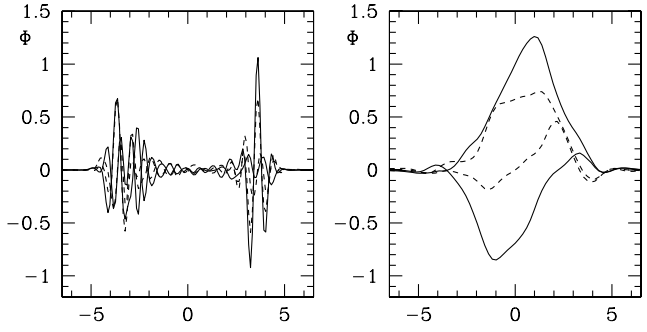

FIG. 4. Typical real (solid) and imaginary (dashed) Φ components of Cowley (left) and Rogers (right) secondaries vs θ. The $k_y = k_y^\ell$ and $k_x = \pm k_y^\ell/2$ components are shown in each.

different. Here, $k_y^{(\ell)}$ is the poloidal wave number of the primary instability. The Rogers secondary has a cutoff at $k_x/k_y^{(\ell)} = 1$, while the Cowley secondary extends to high $k_x/k_y^{(\ell)}$. In the sequel, we consider $k_x/k_y^{(\ell)} = 0.5$ as a representative value.

A central result of this Letter is that ETG turbulence is well characterized as a competition between primary and secondary instabilities. This conclusion rests on the data of Fig. 2. The dashed lines are the predictions of the secondary instability theory for the parameters used in the nonlinear simulations. A single fit parameter (representing the ratio of the normalized heat flux to the normalized Φ) was held fixed for all the points in the figure. A more detailed theory would predict this ratio. Importantly, neither the linear growth rate nor the maximal value of $\gamma/\langle k_\perp^2 \rangle$ predicts the variation found in the nonlinear simulations. For example, the negative shear cases (see Fig. 2) with $R/L_{Te} - R/L_{Tc} > 6$ have maximized $\gamma/\langle k_\parallel^2 \rangle$ values which *exceed* those of the $\hat{s} = 0.8$ cases. It is the variation of the secondary growth rate as the linear eigenfunction changes in response to the equilibrium parameters that correlates with the difference in the nonlinear flux. The secondary growth rates exhibit a strong dependence on magnetic shear as the secondary transitions from a Rogers secondary (moderate positive shear) to a Cowley secondary (negative shear).

Hence, the main variation of the electron heat flux from ETG modes can be accounted for by two physical effects: the degree to which the relatively long wavelength ($k_y \rho_e \sim 0.1$–0.2) primary ETG instabilities contain a significant parallel velocity perturbation, and the proximity of the electron temperature gradient scale length to its critical value. Concerning the second effect, we have derived a formula for the linear threshold of ETG modes in toroidal geometry based on extensive numerical computations [10]. For circular cross section tokamaks with $\hat{s} \gtrsim 0.2$ and $L_n/L_{Te} < 0.8$, we find

$$(R/L_{Te})_{\rm crit} = (1 + \tau)(\mathcal{A} + \mathcal{B}\hat{s}/q) f(\epsilon). \qquad (1)$$

In this expression, $\tau \equiv Z_{\rm eff} T_e/T_i$. Moreover, $\mathcal{A} = 1.33$ and $\mathcal{B} = 1.91$. These values were calculated analytically in the appropriate limiting cases by Romanelli [4] ($\mathcal{A} = 4/3$, $\mathcal{B} = 0$) and Hahm and Tang [11] ($\mathcal{A} = 0$, $\mathcal{B} \approx 1.88$). Romanelli's calculation neglected parallel compressibility, while Hahm and Tang neglected perpendicular compressibility. Our numerical result indicates that a simple linear combination generally works well. Finite inverse aspect ratio corrections due to $\epsilon \equiv r/R \neq 0$ are described by $f(\epsilon)$ with $f(0) = 1$.

We now turn to comparisons of these results with experimental data from the Tore Supra tokamak [12]. In the experiments described in Ref. [12], heating was applied mainly to the electrons. Complications related to rotation, ion energy transport, ion-scale turbulence, and sawteeth were minimized. A clear threshold dependence

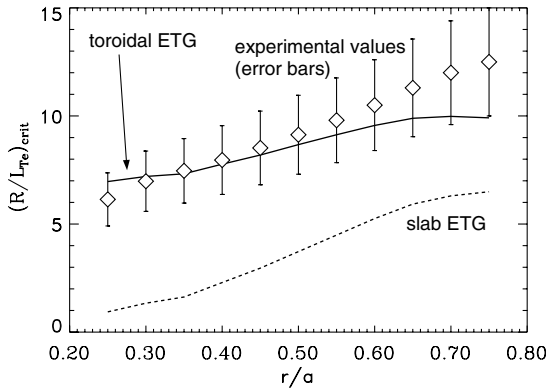

FIG. 5. Critical gradient profile for Tore Supra discharges: experimental results vs predictions for toroidal ETG modes [based on Eq. (1)] and for pure slab ETG modes.

of $\chi_e(R/L_{Te})$ was observed, and a sequence of discharges was used to determine the radial profile and parametric dependence of R/L_{Tc}. In Fig. 5, we demonstrate good agreement between the ETG prediction of Eq. (1) and the experimental results (within the experimental error bars). The theoretically determined values of R/L_{Tc} depend strongly on τ, which has an experimental uncertainty of at least 20%, since $T_i(r)$ and $Z_{\text{eff}}(r)$ were not directly measured. For our comparison, we took a radially constant value of $\tau = 4$. This is a reasonable choice since it reproduces the Hahm-Tang result in Fig. 6 of Ref. [12] (also shown in Fig. 5 here) well, and $Z_{\text{eff}} > 2$, $T_e/T_i \sim 2$ for these hot electron ^{4}He discharges. Direct evaluation of $f(\epsilon)$ for these parameters yields $f(\epsilon) \sim 1 - \epsilon$. Evidently, the threshold of the pure slab ETG mode is experimentally irrelevant. As demonstrated above, perpendicular compressibility (i.e., curvature drive) results in greater ETG transport, and its inclusion brings the theoretical threshold into reasonable agreement with the experimental data. Horton *et al.* [13] argue that this experimental data implies the existence of an Ohkawa-type inverse β scaling of χ_e. However, their analysis depends critically on the assumption that the relevant threshold R/L_{Tc} is given by the Hahm-Tang (slab) expression, and should be reevaluated in light of the results shown in Fig. 5.

Experimentally, χ_e in these discharges is stiff, with $\chi_e \sim 10\rho_e^2 \nu_{te}/L_{Te}$ for $R/L_{Te} - R/L_{Tc} \sim 2$–4. This is in the range of the simulation predictions shown in Fig. 2. Our results therefore suggest that high-amplitude, streamer-dominated ETG turbulence with fluctuation spectra similar to Fig. 3 may be responsible for the core electron energy transport in these Tore Supra discharges, which are nearly ideal for ETG studies. Possible improvements include flatter density profiles (thereby reducing the possible influence of TEMs) and lower values of τ (such that ETG modes set in earlier than TEMs with increasing R/L_{T_e}).

In summary, we presented the first quantitative predictions of transport levels, fluctuation characteristics, and threshold conditions for ETG turbulence. Many state-of-the-art linear (~ 3500) and nonlinear (> 50) gyrokinetic simulations form the basis of these predictions. There are no adjustable parameters, but the effects of electromagnetic fluctuations and of coupling to longer wavelength turbulence deserve further consideration. Comparing our results with experimental data from Tore Supra discharges with dominant electron heating, we find that the experimentally determined critical gradients are described well by the toroidal ETG critical gradient, and that the T_e profile stiffness found experimentally compares favorably with gyrokinetic simulations. Finally, we presented a theoretical model which explains key simulation results quantitatively. This model uniquely includes consideration of two distinct secondary instabilities, giving rise to qualitative differences in the slab and toroidal limits. It may well provide a useful conceptual framework for a more detailed analytical description of this and other plasma turbulence problems.

We thank J.W. Connor, S.C. Cowley, G.W. Hammett, G.T. Hoang, B.N. Rogers, and F. Ryter for valuable discussions, and the Plasma Microturbulence Project for support. The computations were performed at the Leibniz Computing Center, at the Garching Computing Center, and at the National Energy Research Scientific Computing Center.

[1] See, for example, D.W. Ross *et al.*, Phys. Plasmas **9**, 177 (2002).
[2] F. Jenko, W. Dorland, M. Kotschenreuther, and B.N. Rogers, Phys. Plasmas **7**, 1904 (2000).
[3] W. Dorland, F. Jenko, M. Kotschenreuther, and B.N. Rogers, Phys. Rev. Lett. **85**, 5579 (2000).
[4] F. Romanelli, Phys. Fluids B **1**, 1018 (1989).
[5] B.B. Kadomtsev, *Plasma Turbulence* (Academic, London, 1965).
[6] S.C. Cowley, R.M. Kulsrud, and R. Sudan, Phys. Fluids B **3**, 2767 (1991).
[7] E.A. Frieman and L. Chen, Phys. Fluids **25**, 502 (1982).
[8] M.A. Beer, S.C. Cowley, and G.W. Hammett, Phys. Plasmas **2**, 2687 (1995).
[9] J.W. Connor, R.J. Hastie, and J.B. Taylor, Phys. Rev. Lett. **40**, 396 (1978).
[10] F. Jenko, W. Dorland, and G.W. Hammett, Phys. Plasmas **8**, 4096 (2001).
[11] T.S. Hahm and W.M. Tang, Phys. Fluids B **1**, 1185 (1989).
[12] G.T. Hoang *et al.*, Phys. Rev. Lett. **87**, 125001 (2001).
[13] W. Horton *et al.*, Phys. Plasmas **7**, 1494 (2000).